Journal of Inflammation Research

Dovepress
Taylor & Francis Group

Open Access Full Text Article

ORIGINAL RESEARCH

Inflammation-Induced Nitric Oxide Synthase May Mediate the Acute Hypotensive Effect of ST36 Stimulation

Qiu-Lian Lei[1,2,*], Xing Yue[2,*], Xiao-Xiang Sun[2], Li-Juan Zhu[2], Shuqing Liu[2], Hao Hong[3], Zili Tang[2], Xin Cao[2,4]

[1]The Affiliated Hospital of Chengdu University of Traditional Chinese Medicine, Chengdu University of Traditional Chinese Medicine, Chengdu, Sichuan, People's Republic of China; [2]Acupuncture and Tuina School, Chengdu University of Traditional Chinese Medicine, Chengdu University of Traditional Chinese Medicine, Chengdu, Sichuan, People's Republic of China; [3]Dushu Lake Hospital Affiliated to Soochow University, Soochow University, Suzhou, Jiangsu, People's Republic of China; [4]Acupuncture and Chronobiology Key Laboratory of Sichuan Province, Chengdu University of Traditional Chinese Medicine, Chengdu, Sichuan, People's Republic of China

*These authors contributed equally to this work

Correspondence: Xin Cao; Zili Tang, Acupuncture and Tuina School, Chengdu University of Traditional Chinese Medicine, Wenjiang District, Chengdu, Sichuan, 611137, People's Republic of China, Tel +86-28-87526671, Fax +86-28-61800000, Email caoxin@cdutcm.edu.cn; tangzili@cdutcm.edu.cn

Purpose: Acupoint Zusanli (ST36) has been shown to reduce blood pressure, but the underlying mechanism remains unknown. This study aimed to characterize the effects of manual acupuncture (MA) at ST36 on BP and its associated mechanisms in anesthetized rats.

Methods: The cardiovascular response to MA at ST36 in Sprague-Dawley rats was measured by electrocardiogram, hemodynamic methods, heart rate variability, echocardiography, laser speckle contrast imaging, and Western blotting. RNA sequencing was employed for mechanistic investigation, and validation was performed through blood enzyme-linked immunosorbent assay and pharmacologic inhibition.

Results: Stimulation of ST36 increased peripheral blood flow while decreasing the velocity time integral of the femoral artery and cardiac stroke volume. This stimulation induced transient hypotension, accompanied by a decreased heart rate and reduced cardiac contractility, thereby exerting negative chronotropic and inotropic effects on the heart. Furthermore, the increased low-/high-frequency ratio after ST36 stimulation, along with the upregulation of phosphorylated tyrosine hydroxylase, indicated sympathetic activation. RNA sequencing at the local acupoint revealed enrichment of inflammation-related pathways following ST36 stimulation, which was corroborated by elevated tumor necrosis factor-alpha (TNF-α) levels in the serum. Notably, the nitric oxide synthase (NOS) inhibitor L-NG-Nitro arginine methyl ester (L-NAME) effectively suppressed the induced hypotension.

Conclusion: These results indicated that MA at ST36 induced inflammation, which activated NOS and resulted in the release of nitric oxide. This led to the vasodilation of peripheral vessels and transient hypotension.

Keywords: ST36, manual acupuncture, autonomic nervous system, nitric oxide synthase, TNF-α

Introduction

Acupuncture, as an alternative medicine, has been acknowledged by the World Health Organization for treating some specific diseases, including hypertension.[1] Many clinical randomized controlled trials have reported that acupuncture can lower BP, particularly with the frequent application ST36.[1–4] Anatomically located near common peroneal nerve, ST36 region contains fibres innervating the deep fascia.[5] Unlike electroacupuncture (EA) that primarily involves current stimulation, MA employs basic needle handling techniques, such as lifting-thrusting (提插) and twisting-rotating (捻转), to exert therapeutic effects by causing tissue deformation and local inflammation. Previous study has shown that MA at ST36 increased microvascular perfusion, decreased BP and heart rate, and significantly improved heart rate variability (HRV) in healthy volunteers.[6] This observed hypotensive effect is commonly attributed to neuromodulation, specifically

Received: 18 September 2024
Accepted: 15 February 2025
Published: 26 February 2025

mediating vagal reflexes evoked by the common peroneal nerve.[7,8] However, an animal experiment found that cutting both sides of vagus nerve could not abolish the hypotensive pressure of ST36 in anesthetized rats, suggesting the involvement of additional mechanisms.[9]

Nitric oxide (NO) is an important mediator proposed to contribute to the hypotensive effect observed with long-term stimulation of ST36.[10–12] NO is endogenously synthesized by nitric oxide synthase (NOS) enzyme in endothelial cells, where it oxidizes L-arginine to L-citrulline in the presence of oxygen and nicotinamide adenine dinucleotide phosphate. Three isoforms of NOS have been identified: neuronal NO synthase (nNOS or NOS1), inducible NO synthase (iNOS or NOS2) and endothelial NO synthase (eNOS or NOS3).[13] Once produced, NO diffuses rapidly into adjacent smooth muscle cells, where it activates soluble guanylate cyclase, resulting in elevated cyclic guanosine monophosphate (cGMP) levels. The increase in cGMP activates protein kinase G, leading to reduced intracellular calcium levels and activation of myosin light chain phosphatase, resulting in smooth muscle relaxation, vasodilation, and subsequently lowered BP. Pharmacological inhibition of NOS activity, particularly through the use of L-NG-Nitro arginine methyl ester (L-NAME), has been extensively studied both in vitro and in vivo.[14,15] Jana K et al demonstrated that both acute and chronic L-NAME treatment induces alterations in BP and vascular reactivity due to decreased NO bioavailability.[16] Kenichi K et al reported that local administration of L-NAME attenuated cutaneous vasodilation following acupuncture stimulation compared to control sites in humans.[17] It is postulated that manual acupuncture (MA) at ST36 may induce an inflammatory response, which could upregulate iNOS, thereby facilitating NO production. However, the involvement of NO in the hypotensive effects of ST36 remains to be elucidated, and no study has comprehensively investigated the underlying mechanisms through which MA at ST36 modulates BP.

In this study, we sought to characterize the effects of MA at ST36 on BP using electrocardiogram (ECG), hemodynamic tests, echocardiography, and laser speckle contrast imaging (LSCI). Furthermore, we investigated the underlying mechanisms of ST36 on BP through transcriptome analysis and validated the findings via pharmacological inhibition experiments.

Materials and Methods

Experimental Ethics and Animals

Male Sprague-Dawley (SD) rats were purchased from DaShuo Animal Science and Technology Co. Ltd (Chengdu, Sichuan, China). The rats were housed at a constant temperature (23 ± 1 °C) under a 12/12-h light-dark cycle, with free access to food and water. All procedures were approved by the Ethics Committee for Animal Care and Use in Chengdu University of traditional Chinese Medicine (2018–11). Rats were randomly allocated to the MA group (n = 6, ST36), L-NAME group (n = 6), and Saline group (n=6).

The rats were initially anesthetized with 4% isoflurane (Shandong Antemuye, Co., Ltd., Shandong, China) vaporized with room air in a chamber. Once unconscious, they were immediately attached to the anesthetic machine via masks with 2% isoflurane. After intubation, the rats began inhaling 1–1.5% isoflurane vaporized with room air using a volume limited ventilator (Shanghai Alcott Biotech Co., Ltd., Shanghai, China). The surface lead II ECG was obtained from the limb electrodes. The right femoral vein was cannulated for drug administration, and the right femoral artery was cannulated to measure BP. The right internal carotid artery was retrogradely inserted into the left ventricle to measure the left ventricular pressure (LVP). When the cannula was inside the ventricle, diastolic BP declined to about 0 mmHg. Each measurement of ECG, BP and LVP was taken as the mean of three recordings of consecutive complexes. All groups underwent the same anesthesia protocol to ensure consistency, and all data were collected with isoflurane of 1–1.5% after blood pressure and heart rate had stabilized for a minimum of 10 minutes.

Interventions

After a basal assessment, Hwato brand disposable acupuncture needles (size Φ 0.25×40 mm, Suzhou, China) was utilized. ST36 located approximately 5 mm below the fibular head.[18] The manipulation involved lifting, thrusting, twisting, and rotating the needle for 5 minutes (Figure 1A).[19]

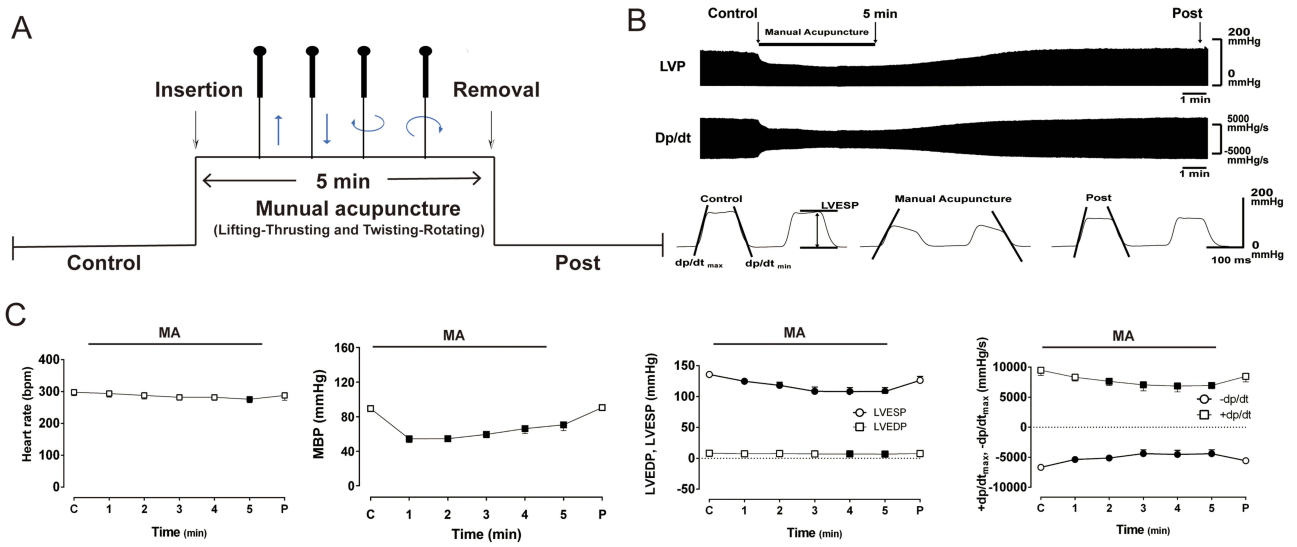

Figure 1 Manual acupuncture (n=6) at Zusanli (ST36) produced a transient hypotension, exerting a negative inotropic and chronotropic effect. (**A**) Schematic representation of a rat treated with MA at ST36. (**B**) Representative LVP, and dp/dt before and after MA at ST36. Typical trace of LVP at pre- (Control), 3 min during stimulation (3 min) and post-manual stimulation (Post). Note the great reduction in LVP and dp/dtmax after manual stimulation. (**C**) Time course of changes in heart rate, MBP, LVEDP, LVESP and dp/dt pre and post ST36 stimulation. Data are presented as mean + SD. Solid symbols represent significant difference when compared with control variable.
Abbreviations: MA, manual acupuncture; MBP, mean blood pressure; LVP, left ventricular pressure; LVEDP, left ventricular end systolic pressure; LVESP, left ventricular end systolic pressure.

L-NAME (Jinyao, Ltd., Tianjin, China) was dissolved in 0.9% saline (Sichuan Kelun Pharmaceutical Research Institute Co., Ltd, Chengdu, China) at a concentration of 0.04 mg/mL and administered intravenously. The effects of the vehicle (saline) alone were examined by the same protocol as for the drug assessment.

HRV Analysis

All rats were anesthetized in the chamber with 4% isoflurane, then carefully positioned on the ECG recording platform and attached to masks under 1.5% isoflurane. A cannula was inserted into the trachea and the rats began inhaling 1%-1.5% isoflurane vaporized with room air using a volume limited ventilator. A surface lead II ECG was obtained. During the experiment, ventricular rhythm was continuously recorded using a PowerLab system (AD Instruments, Australia) at a sampling rate of 1 kHz. After recording the baseline rhythm for about 20 minutes, ST36 stimulation was performed. HRV analysis was recorded 5 minutes before and after ST36 stimulation. The records were processed using labchart 8.2.3 (AD Instruments, Australia). Ectopic ventricular beats were excluded from the analysis.

Discrete Fourier transformation was used for the analysis of the time and frequency domain parameters. Time-domain analysis was performed over a 5-minute period by assessing root mean square of successive difference (RMSSD). Analysis of the power spectra was performed on two frequency ranges, revealing a low frequency (LF) component between 0.2 hz and 0.75 hz and a high frequency (HF) component between 0.75 hz and 2.50 hz. Power spectral analysis of HRV has been used as a sensitive indicator of autonomic nervous system activity. LF domain power generally reflects both the sympathetic and parasympathetic nervous systems. HF domain power generally reflects the parasympathetic nervous system. The LF/HF ratio, which reflects the balance between the sympathetic and parasympathetic nervous systems, was calculated. A high ratio indicates greater sympathetic activity, and a low ratio indicates greater parasympathetic activity. Comparative analysis of RMSSD, LF, HF and LF/HF ratios before and after ST36 stimulation were conducted twice, with or without atropine infusion, to evaluate whether the vagal nerve is involved.

Echocardiography

All rats were subjected to transthoracic echocardiography under 1.5% isoflurane anesthesia to characterize the effects of ST36 on cardiac structure and function. Echocardiography was performed with an ultrasound system (Vevo 3100 imaging digital ultrasound system, VisualSonics, FUJIFILM VisualSonics, Inc., Canada), equipped with a 13–24 MHz

https://doi.org/10.2147/JIR.S494037

(MS250D) transducer probe. A longitudinal view of a straight arterial segment was imaged for volumetric measurement, avoiding sites of vascular bifurcation. The wall filter was set at 50.0 hz, and the sample volume was set to encompass the entire lumen to ensure that slow-moving blood flow was included. The beam was positioned with the angle of insonation set no greater than 60° to measure time-averaged mean velocity. Doppler signal recorded at femoral artery was used to measure peak velocity and its VTI.

Western Blotting (WB) Analysis

Protein samples were extracted from aorta tissues by preparing in cold RIPA lysis buffer (MB-030-0050, Multi-Sciences Biotech, Hangzhou, Zhejiang, China) containing complete protease inhibitor cocktail (11697498001, ROCHE, Switzerland) and phosphatase inhibitor (4906837001, ROCHE, Switzerland). Protein samples were separated by SDS-polyacrylamide gel electrophoresis and transferred to the 0.22 μm PVDF membrane (PI88520, Millipore, USA), which were detected using specific primary antibody (anti-TH, 1:1000, 2792, Cell Signaling Technology, USA; anti-p-TH, 1:1000, 2791, Cell Signaling Technology, USA; anti-AChE, 1:1000, PA5-95250, Invitrogen, USA). Bound antibodies were detected using rabbit peroxidase-conjugated secondary antibody and visualized by enhanced chemiluminescence (RK-18-8816-31, Multi-Sciences Biotech, China) in the chemiluminescence imaging system (Chemi Scope 6100, Clinx Science Instruments, Shanghai, China). Band intensity was quantified using Image J (National Institute of Health, USA).

Laser Speckle Contrast Imaging

The rats were anesthetized with 3% isoflurane, placed on a stereotaxic apparatus (RWD Life Technology, Shenzhen, China), and maintained with 1.5–2.0% isoflurane via mask at a speed of 0.5 L/min. After shaking off the hair in the groin, the LSCI system (Wuhan SIM Optoelectronics Technology Co., Wuhan, China) consisting of an Olympus ZS61 microscope, a continuous wavelength laser diode (λ=785 nm), and a charge-coupled device camera, were used. The groin area was illuminated vertically by the continuous wavelength (λ=785 nm) laser source, and the images reflected by the biological tissue were captured by an in-system CCD imaging system. A random interference pattern is created due to the mutual interference of scattered light through different optical paths, and a pseudo-color image is generated by computer processing automatically. The configuration of blood vessels and the direction of blood flow on the surface were examined under a microscope. The blood flow index (BFI) reflected by the gray average value of the blood flow image was examined and calculated by Image J software. All the rats were kept warm during the test and then housed in a single cage after awakening with access to food and water.

RNA Sequencing and Data Analysis

The skin samples were collected immediately after the acupuncture stimulation at ST36 was completed. RNA was extracted from the skin at the acupoint ST36 of rats in each group, and RNA integrity was assessed using the RNA Nano 6000 Assay Kit of the Bioanalyzer 2100 system (Agilent Technologies, CA, USA). The RNA-seq library was prepared using the TruSeq RNA Sample Preparation kit v2 (Illumina, 15,025,062) according to the manufacturer's instructions. A cBot Multiplex re-hybridization plate and TruSeq SBS kit V3 (Illumina, 15,021,668) were used for cluster generation. Sequencing was performed using Illumina Novaseq 6000 (Illumina, USA).

For data analysis, raw data (raw reads) of fastq format were firstly processed through in-house Perl scripts. Clean reads were then aligned to rat genome sequences using Hisat2 v2.0.5 mapping tool.[20] The mapped reads were then assembled by StringTie (v1.3.3b)[21]. FeatureCounts v1.5.0-p3 was used to count the reads numbers mapped to each gene and these counts were normalized by FPKM (fragments per kilobase of transcript per million fragments mapped) for gene expression qualification. Differential expression analysis was performed using the DESeq2 R package (v1.20.0). Significant differentially expressed genes (DEGs) were identified using the following selection criteria: |log2 fold change (FC)| > 0 and false discovery rate (FDR) < 0.05. Gene Ontology (GO) analysis and KEGG (Kyoto Encyclopedia of Genes and Genomes) enrichment pathways were then performed as previously described.[22] To validate KEGG pathway enrichment results, Gene Set Enrichment Analysis (GSEA) was conducted using the clusterProfiler package (v4.14.4).[23] Enrichment scores were computed using 1000 permutations, and statistical significance was determined by normalized enrichment scores (NES ≥ 1.5) and FDR q-values <0.05 (Benjamini-Hochberg correction). Key enriched pathways were

visualized using the enrichplot package (v1.26.5).[24] The RNA-seq data is deposited in the Bioproject database in NCBI, and the BioProject ID is PRJNA1146793.

Cytokine Determination by Blood Enzyme-Linked Immunosorbent Assay

Blood supernatant protein concentration was measured by enzyme-linked immunosorbent assay kits for TNF-α (R0201- 8, Nuohe Bio, Chengdu, China), TGF-β (R0301), IL-1β (R0301), and IL-6 (R0302) to detect expression levels.[25] These assays were carried out according to the instructions provided by the manufacturer. Each sample was detected at least three times.

Statistical Analysis

All data are presented as mean ± standard deviation (SD). For ECG and hemodynamic variables, statistical analysis was done using one-way analysis of variance (ANOVA) with the Turkey test using GraphPad Prism 9.3 (GraphPad Software Inc., La Jolla, CA, USA). For WB, statistical analysis was carried out by the two-tailed, unpaired Student's *t*-test. For HRV between before- and after-acupuncture stimulation, the two-tailed, paired Student's *t*-test was applied. For comparison between control and L-NAME group, two-way repeated measurements were carried out. A value of $P < 0.05$ was considered as statistically significant.

Results

MA at ST36 Acutely Lowered Blood Pressure and Reduced Myocardial Contractility

To characterize the effects of ST36 on cardiac function, we comprehensively recorded electrophysiology and hemodynamic variables in MA conditions. After MA at ST36, BP was reduced, accompanied by a reduction in the left ventricular end-systolic pressure, as well as decreases in +dp/dtmax and -dp/dtmin, and heart rate, exerting negative inotropic and chronotropic effects (Figure 1B and C). Neiguan (PC6), located on the lateral aspect of the lower forearm between the radius and ulna, was also stimulated to verify the specificity of acupoints sine it is frequently used for cardiovascular diseases. However, MA at PC6 hardly altered those cardiovascular variables (Suppl Figure 1).

MA at ST36 Increased Peripheral Blood Flow, and Decreased Stroke Volume

Arterial pressure directly corresponds to peripheral vascular resistance, cardiac output (CO), and arterial elasticity. Approximately 70–90% of the overall peripheral resistance in the circulatory system arises from the microcirculation. Consequently, we employed LSCI to assess peripheral blood perfusion in the ipsilateral groin region adjacent to the acupoint, as well as in the contralateral groin area distal to the acupoint during ST36 stimulation. Our investigation revealed that MA at ST36 significantly enhanced local blood perfusion not only in the ipsilateral groin region (Suppl Figure 2A) adjacent to the acupoint but also in the contralateral groin area (Figure 2A and B). Concurrently, echocardiographic analysis demonstrated a reduction in the velocity time integral (VTI) of the femoral artery (Figure 2C and D) as well as a decrease in cardiac stroke volume (Figure 2E and F). Given that stroke volume is dependent on venous return, this suggests that stimulation of ST36 induced peripheral vasodilation, thereby diminishing venous return. However, these modulatory effects were transient, immediately following the cessation of acupuncture stimulation (Figure 2F). Additionally, the specificity of the acupoint was assessed by examining the effects of MA on peripheral blood perfusion at ST39 (located on the lateral aspect of the lower leg, posterior to the fibula, approximately 6 mm distal to ST36). It was observed that MA at ST39 augmented blood perfusion in the ipsilateral groin region, but did not elicit a similar response in the contralateral groin area.

MA at ST36 Increased LF/HF Ratio

To assess the impact of acupuncture on the autonomic nervous system, RMSSD, LF and HF powers were recorded for five minutes before- and after-ST36 stimulation (Figure 3A). Following ST36 stimulation, there was a significant increase in LF power ($P < 0.05$) (Figure 3B and C) accompanied by a corresponding decrease in HF power ($P < 0.05$) (Figure 3C). The LF/HF ratio, which serves as an indicator of sympathovagal balance, was also calculated and subjected to comparative analysis. We observed a statistically significant elevation in the LF/HF ratio after ST36 stimulation

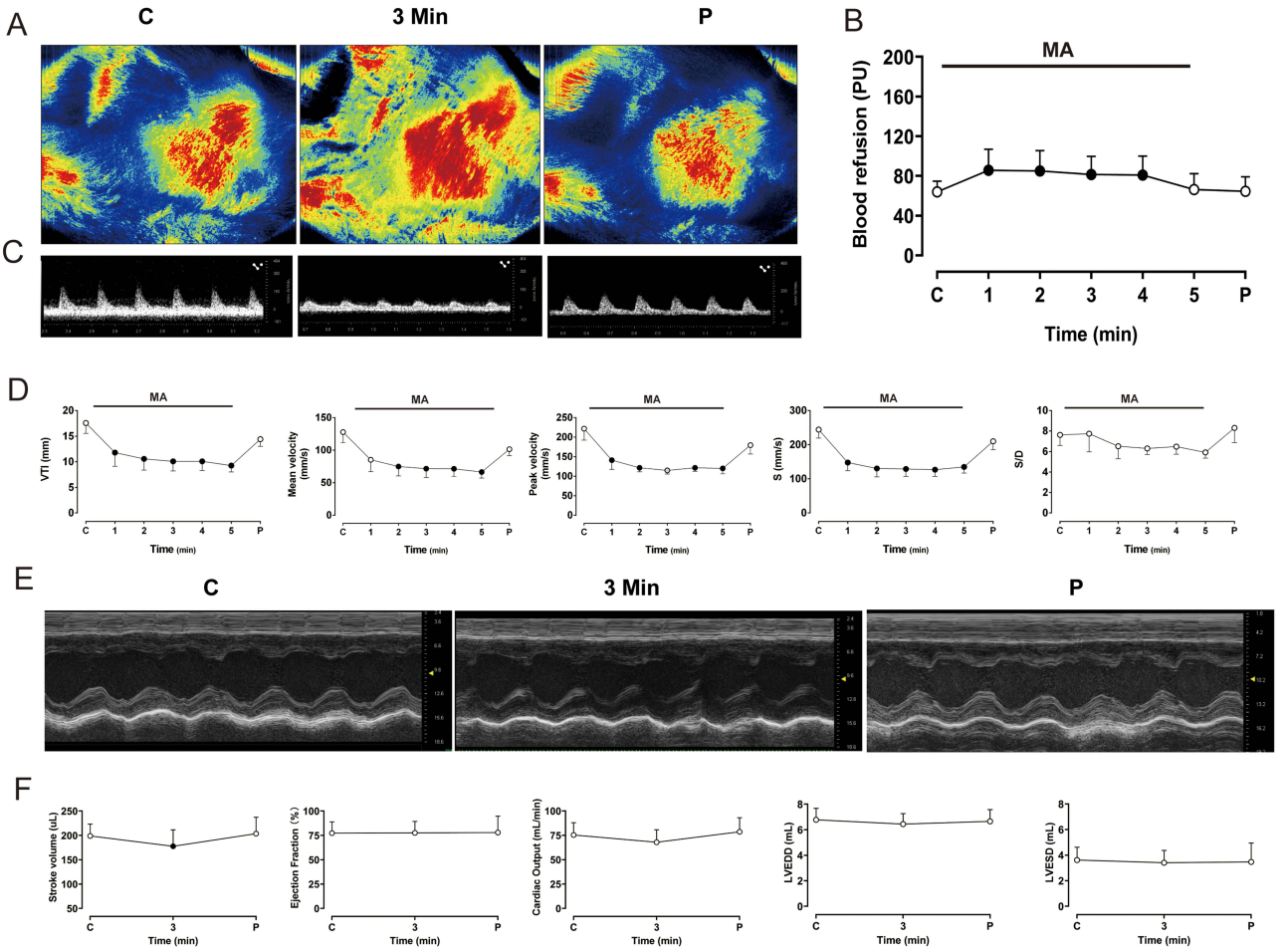

Figure 2 Manual acupuncture at ST36 increased peripheral blood flow and decreased VTI and SV. (**A**) Schematic representation of LSCI images before, during (at 3 min) and post acupuncture stimulation. A significant increase in blood perfusion was observed at three minutes of intervention. (**B**) Manual acupuncture at ST36 increased blood perfusion in opposite groin distal to the ST36 (n=6). (**C**) Representative trace of Doppler images of femoral artery before, during (at 3 min) and post acupuncture stimulation. Echocardiography showed potent decrease of VTI in the femoral artery during manual acupuncture at ST36. (**D**) Manual acupuncture at ST36 decreased VTI, mean velocity, peak velocity, S and D wave and CO during manual acupuncture at ST36 (n=6). (**E**) Representative trace of parasternal long axis images before, during (at 3 min) and post acupuncture stimulation. (**F**) Echocardiography showed decrease of cardiac stroke volume during manual acupuncture at ST36 (n=6). Solid symbols represent significant difference when compared with control variable, P<0.05.

Abbreviations: LSCI, Laser Speckle Contrast Imaging; VTI, velocity time of integral; SV, stroke volume; CO, cardiac output.

relative to the baseline measurements, indicative of enhanced sympathetic nervous system activity ($P < 0.05$). However, there is no statistical significance of RMSSD (Figure 3C).

Upregulation of P-TH/TH After Needle Removal

To further elucidate the impact of acupuncture on the autonomic nervous system, we performed WB analysis. No statistically significant differences were observed in acetylcholinesterase (AChE) and tyrosine hydroxylase (TH) levels in the ventricular tissue between the control group and the ST36-treated group (Figure 4A–C, $P > 0.05$). In contrast, phosphorylated TH (p-TH) levels (Figure 4D, $P < 0.01$) and the p-TH/TH ratio (Figure 4E, $P = 0.067$) were markedly elevated in the ST36-treated group compared to the control group, suggesting an upregulation of sympathetic nervous system activity.

Transcriptome Analysis Revealed Inflammatory Response as the Key Player

To elucidate the underlying mechanisms of the MA effect at ST36 on BP, we performed transcriptome analysis comparing the control and ST36 groups (n=3 per group). The boxplot illustrates the distribution of gene expression

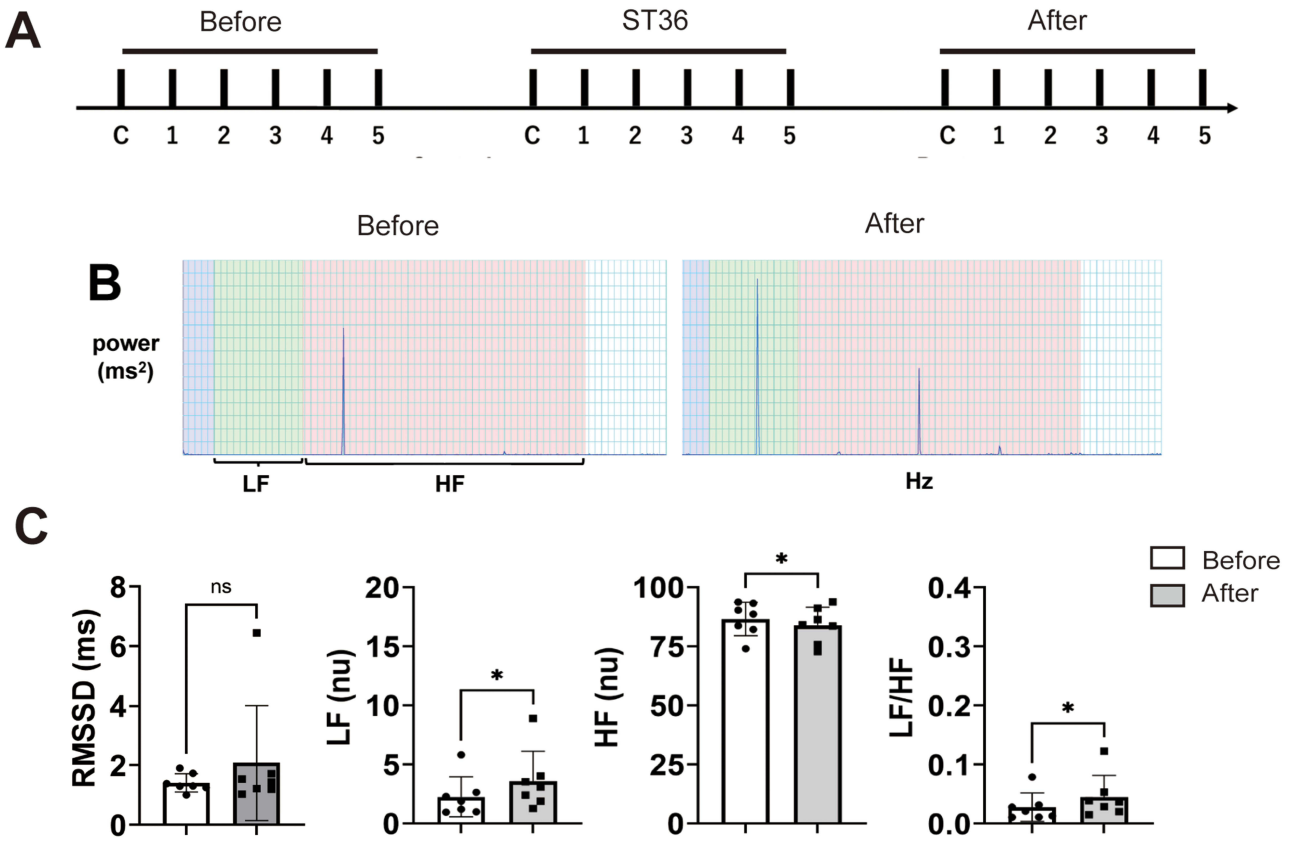

Figure 3 Manual acupuncture at ST36 increased LF/HF ratio. (**A**) Timetable of a rat with HRV analysis before and post manual acupuncture at ST36. (**B**) Representative traces of LF and HF within 5 minutes before- and after-ST36 stimulation. (**C**) Statistical analysis of LF, HF, and LF/HF ratio 5 minutes before- and after-ST36 stimulation (n=6). Statistical significance was defined as $P < 0.05$ (*).

Abbreviations: HRV, Heart rate variability; LF, low frequency; HF, high frequency; LF/HF, low frequency/ high frequency.

levels [log2(FPKM+1) transformed] across different samples (Suppl Figure 3A). Pearson correlation analysis indicated good sample replications (R2 ≥0.89, Suppl Figure 3B). After normalization and $\log_2$-transformation, a total of 12869 genes were mapped, with 11996 genes overlapping between the two groups (Suppl Figure 3C). Applying a cutoff criterion ($|\log_2 FC| > 0$ and P-value < 0.05), we identified 800 DEGs in the ST36 group compared to the control group, with 515 up-regulated genes (Additional file 1) and 285 down-regulated genes (Additional file 2) displayed in a volcano plot (Figure 5A). Strikingly, a large number of these DEGs are involved in the modulation of inflammation, including chemokines (eg, Ccl2, Ccl22, Cxcl1, Cxcl2), interleukins (eg, Il1b, Il10ra, Il17re, Il1rl1), and NOS (Nos1, Nos2, Nostrin). The different expression pattern with hierarchical clustering is shown in the heatmap (Figure 5B). GO function and KEGG pathway enrichment analyses were further performed to comprehensively understand the function of these DEGs. Three GO categories of biological process (BP, blue), cellular component (CC, green), and molecular function (MF, red), with the number of genes annotated in each, are summarized in Figure 5C. In the BP category, inflammatory response and immune regulation are the predominate functions. In the CC and MF categories, extracellular matrix and chemokine activity/receptor binding are notable, respectively. KEGG results showed that TNF signaling pathway, IL-17 signaling pathway, and cytokine-cytokine receptor interaction were enriched among the top 20 pathways (Figure 5D), suggesting a pivotal role of inflammatory response to MA. GSEA analysis was conducted to further validate the enrichment results obtained from KEGG pathway analysis, without relying on predefined cutoff thresholds. The GSEA results corroborated the KEGG findings, highlighting key pathways, including the TNF signaling pathway, IL-17 signaling pathway, and cytokine-cytokine receptor interaction (Figure 5E), in the transient hypotension induced by acupuncture manipulation.

https://doi.org/10.2147/JIR.S494037

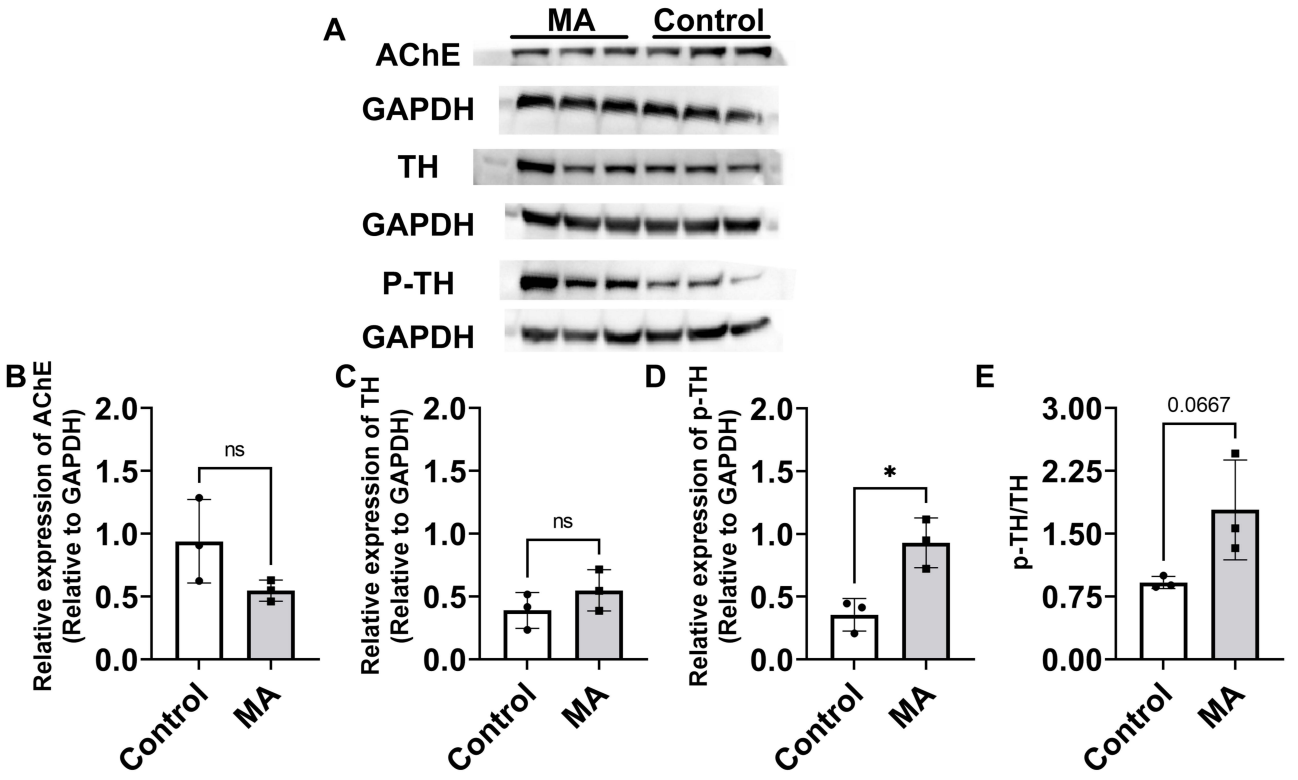

Figure 4 P-TH was upregulated after removal of the needle. (**A**) Left ventricular expression of AChE, TH, and p-TH proteins in the manual acupuncture group and the control group. (**B–E**) Bar graphs presenting the statistical analysis of AChE, TH, p-TH, and p-TH/TH (n=3). Statistical significance was defined as $P < 0.05$ (*).
Abbreviations: AChE, acetylcholinesterase; TH, tyrosine hydroxylase; p-TH, phosphorylated tyrosine hydroxylase; MA, manual.

Based on the transcriptome findings, we examined the expression levels of inflammatory factors (TNF-α, TGF-β, IL-1β and IL-6) in the serum of rats. ELISA results showed a reduction in TGF-β and IL-1β (Suppl Figure 4A–C). Notably, TNF-α level in the serum was significantly elevated after MA at ST36 compared with the control group (Figure 5F). However, the local expression of TNF-α at the acupoint site showed only a modest, non-significant increase of 12%.

NOS Inhibitor Blocked the Hypotensive Effect of MA at ST36

Transcriptome analysis showed inflammatory response elicited after MA as well as elevation of NOS. To elucidate the role of NOS in mediating the hypotensive effect of manual acupuncture (MA) at ST36, we administered L-NAME, a non-selective NOS inhibitor intravenously and evaluated its influence on the ST36-induced cardiovascular response (Figure 6A). The results demonstrated that L-NAME effectively abrogated the hypotensive effect of MA at ST36 (Figure 6B–D), whereas saline (control group) failed to inhibit this response, thereby implicating NO as a mediator of the acupuncture-induced hypotensive effect (Figure 6B–D). Moreover, there were no statistically significant differences in heart rate, dp/dtmax, and dp/dtmin between the L-NAME and saline groups during the intervention (Figure 6B–D). However, the reduction in mean arterial pressure was substantially greater in the L-NAME group compared to the saline group (Figure 6C). These findings suggest that nitric oxide plays a pivotal role in the hypotensive effect elicited by MA at ST36.

Discussion

ST36 is a crucial acupoint employed either individually or in combination with others for the treatment of various disorders through acupuncture. Although substantial research has been conducted on its therapeutic effects, its physiological impacts remain underexplored. In this study, we utilized a multidisciplinary approach to evaluate the physiological and molecular effects to manual acupuncture at ST36. Our findings revealed an acute but transient hypotensive effect. Mechanistic investigation uncovered inflammatory responses, specifically the activation of TNF signaling

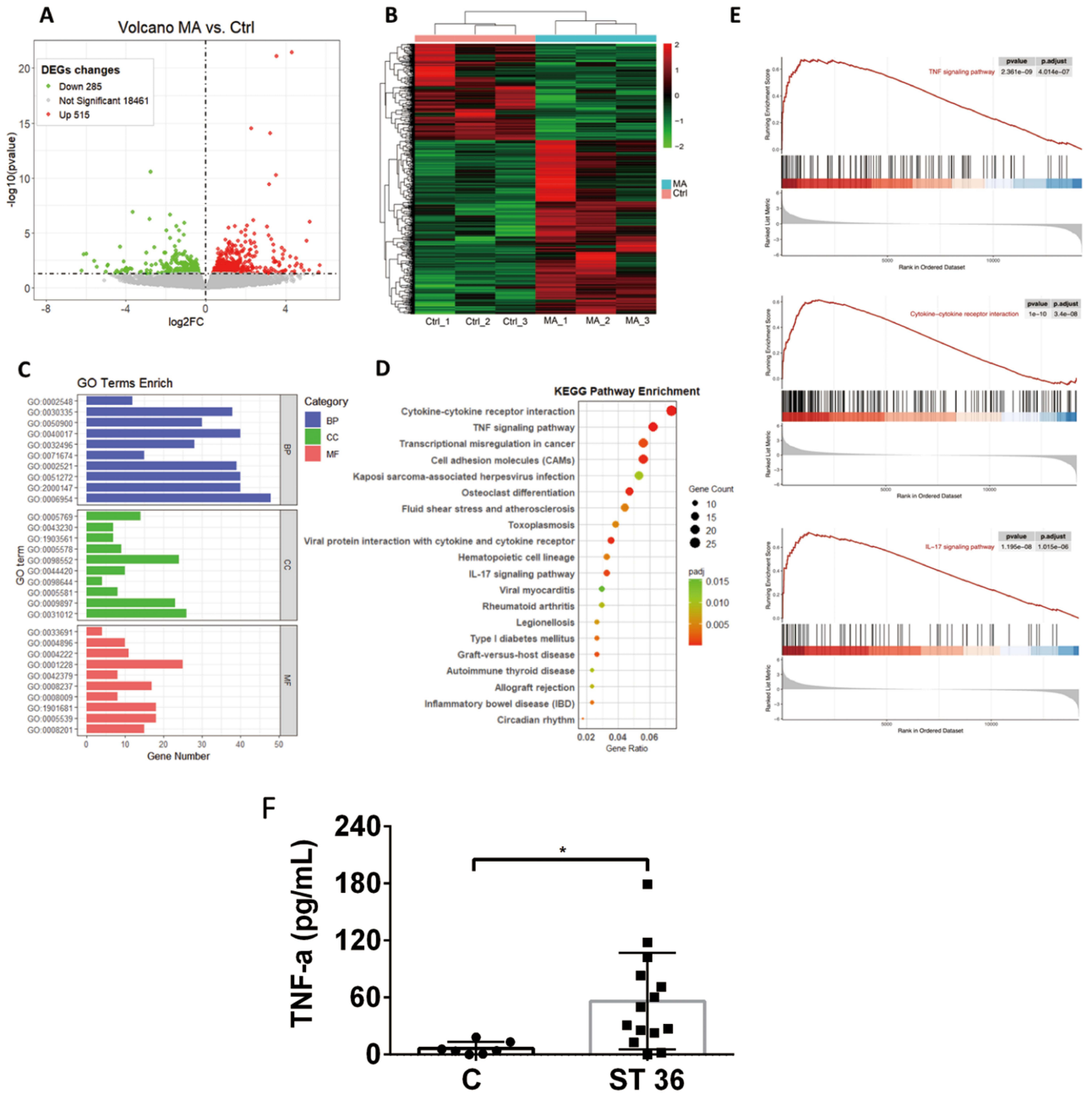

Figure 5 Transcriptome analysis. (**A**) Volcano plot displaying up- and down-regulated DEGs in the ST36 group compared to the control (|log2FC| >0, P-value <0.05). (**B**) Heatmap of hierarchical clustering for DEGs, with notable gene expression patterns. (**C**) GO analysis of biological process (BP, blue), cellular component (CC, green), and molecular function (MF, red) with the number of genes annotated in each GO-term. (**D**) KEGG analysis revealing top 20 enriched pathways among DEGs, with color representing adjusted P-value (Padj) and bubble size indicating the number of genes (n=3 per group). (**E**) GSEA analysis confirmed the enrichment of selected pathways: TNF pathway, IL-17 pathway, and cytokine-cytokine interaction. (**F**) TNF-α was elevated in the serum (n=7 for control group, n=14 for ST36 group). Statistical significance was defined as $P < 0.05$ (*).

Abbreviations: DEG, Differentially Expressed Genes; TNF-α, Tumor Necrosis Factor-alpha.

pathways and upregulation of iNOS. These results suggest that stimulation at ST36 may induce a pro-inflammatory environment, leading to increased iNOS expression and subsequent nitric oxide production, which contributes to the observed reductions in blood pressure and sympathetic activation (Figure 7).

Upon initiation of manual acupuncture, we observed a pronounced and transient decrease in BP, accompanied by reductions in heart rate, left ventricular pressure, and both $+dp/dt_{max}$ and $-dp/dt_{min}$. This transient effect may be associated with the brief local stimulation generated by the hand-needle lifting and twisting technique. In particular,

https://doi.org/10.2147/JIR.S494037

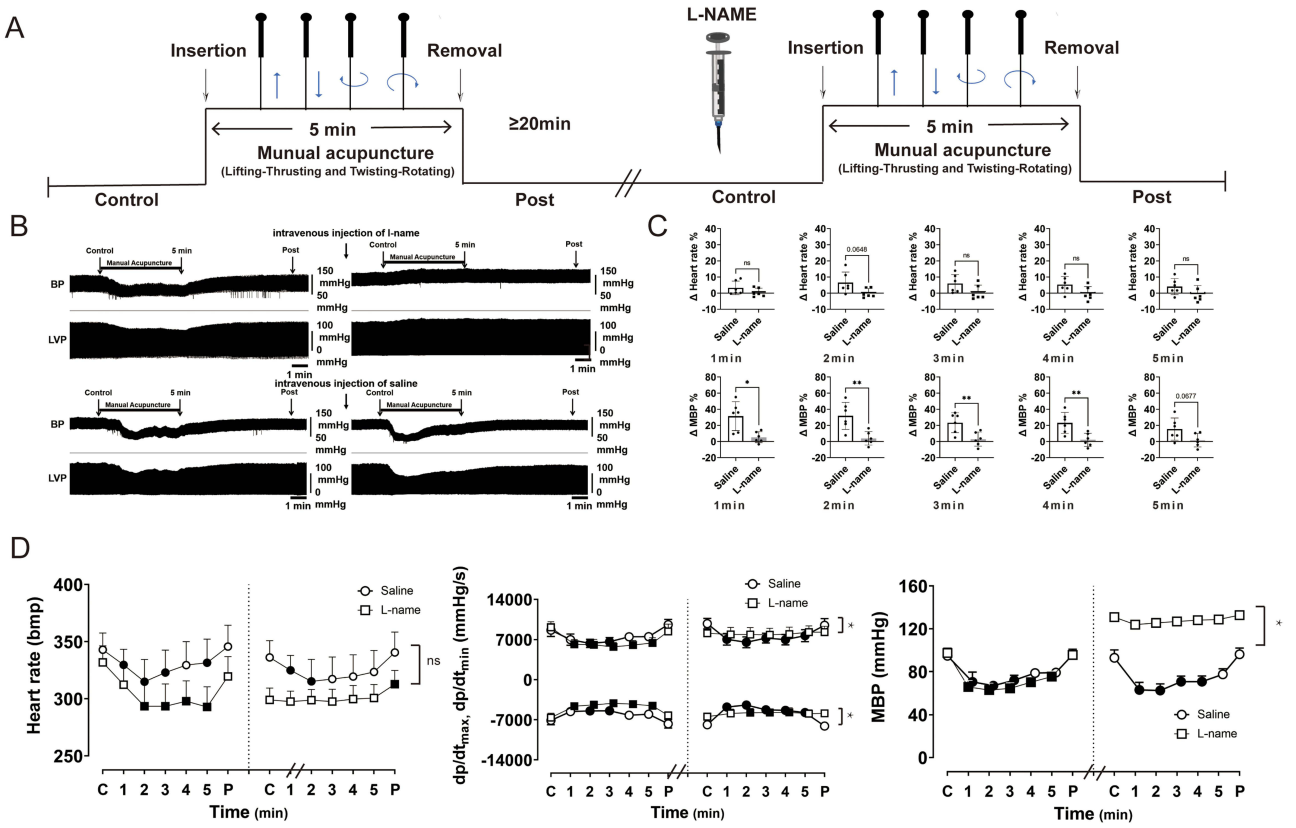

Figure 6 L-NAME abolished the hypotensive effect of manual acupuncture at ST36. (**A**) Schematic representation of a rat treated with manual acupuncture at ST36 before and after administration of L-NAME. (**B**) Representative traces of blood pressure and left ventricular pressure of a rat treated with L-NAME. Before administration of L-NAME, ST36 induced a potent hypotensive effect, however, L-NAME eliminated it. (**C**) Comparisons of Δ heart rate (upper panel) and ΔMBP (lower panel) between saline and L-NAME group. *P<0.05, **P<0.01, (n=6 for saline group and n=6 for L-NAME group, unpaired *T* test for comparisons of saline and L-NAME). Δheart rate %=(Heart rate Control-Heart rateMA)/ Heart rate Control. Δ MBP %=(MBPControl-MBPMA)/ MBP Control. (**D**) Time course of changes in heart rate, dp/dtmax and -dp/dtmin, mean blood pressure before and after L-NAME injection. Solid symbols represent significant difference when compared with control variable, P<0.05. (n=6 for Saline group and n=6 for L-NAME group. One-way analysis of variance (ANOVA) with Turkey corrections was performed. Data are presented as mean ± standard deviation. Statistical significance was defined as P < 0.05 (*).

Abbreviations: L-NAME, L-NG-Nitro arginine methyl ester; MBP, mean blood pressure; LVP, left ventricular pressure.

during the initial few minutes of manipulation, mechanical stimulation induced by acupuncture may trigger a localized inflammatory response and stretch the tissue, and thus regulate vasomotor function through the release of bioactive substances, such as NO and adenosine. However, as the manipulation ends or the stimulation weakens, the local response gradually diminishes, leading to a reduction in the hypotensive effect. To further elucidate the effects of ST36 on BP, echocardiographic assessments were performed on the ventricle and femoral artery. A decrease in cardiac stroke volume and the VTI of the femoral artery was detected. However, the drop in VTI and stroke volume is temporary, and both parameters return to normal levels within five minutes after removing the acupuncture stimulus (Figure 2D and F). Transient cutaneous vasodilation, assessed by Laser Speckle Contrast Imaging, supports this observation. Following the termination of acupuncture, BP, heart rate, and contractility returned to baseline levels within five minutes, accompanied by an upregulation of p-TH, p-TH/TH, and increases in the LF/HF ratio of heart rate variability. The elevation in p-TH/TH and LF/HF ratios suggests enhanced sympathetic activity, potentially as a reflexive response to ST36-induced vasodilation. When BP drops excessively, the rate of baroreceptor firing diminishes, likely triggering an increase in sympathetic stimulation of the heart, thus restoring BP, heart rate, and contractility to baseline levels.

The acute effects of acupuncture at PC6 and ST39 on BP and peripheral blood flow were also assessed to determine acupoint specificity, respectively. We found that manual acupuncture at PC6 did not reduce LVP and cardiac contractility (Suppl Figure 1). ST39 increased ipsilateral blood flow (Suppl Figure 2B), but did not increase contralateral blood flow (Suppl Figure 2C) as observed with ST36, suggesting that the cardiovascular responses are specific to ST36. Although

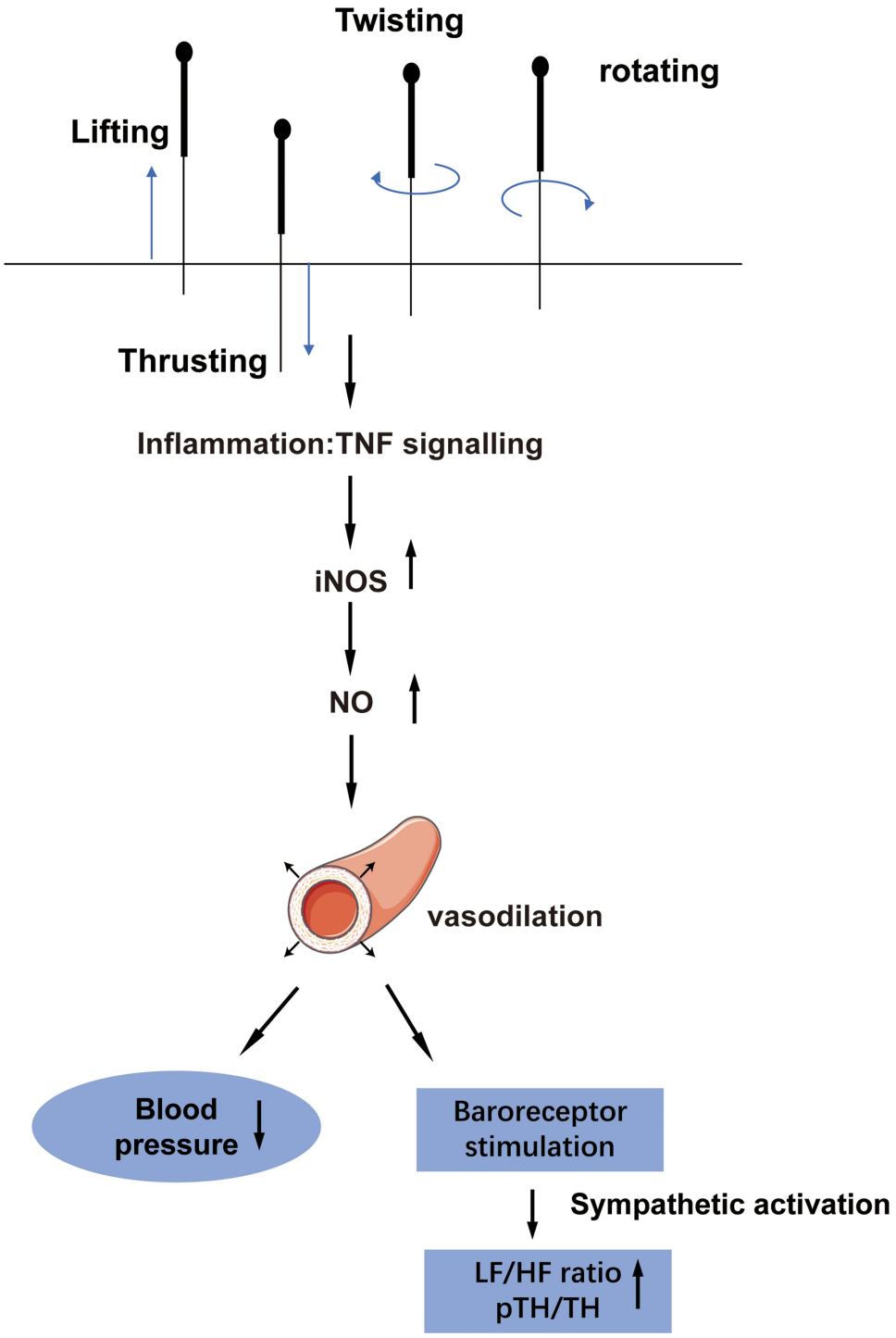

Figure 7 ST36 stimulation created a pro-inflammatory environment, inducing iNOS expression and NO production, which leads to decreased BP and sympathetic activation.
Abbreviations: Inos, inducible nitric oxide synthase; NO, nitric oxide.

previous studies have reported acupuncture at PC6 lower BP in spontaneously hypertensive rats[26] and its role in cardiac regulation via sympathetic activation in myocardial ischemia models,[27] the discrepancy with our findings likely arises from differences in experimental design. Specifically, we used healthy SD rats rather than disease models, which may influence acupoint response. Moreover, our earlier study in an anesthetized canine hypertension model demonstrated that acupuncture at clinically common acupoints such as Taichong (LR3) and Renying (ST9) increased mean BP (Cao et al,

https://doi.org/10.2147/JIR.S494037

2015). This further highlights the importance of experimental context in determining acupuncture's cardiovascular effects. Collectively, our findings emphasize the specificity of ST36 in eliciting BP-lowering responses, distinguishing it from PC6 and ST39 under the conditions tested.[28]

We conducted transcriptomic analysis to investigate the mechanisms behind peripheral vasodilation and hypotensive effect observed during acupuncture. The results revealed the enrichment of inflammation-related signaling pathways, such as TNF signaling, in the acupoint area. TNF-α is a pro-inflammatory cytokine implicated in the pathogenesis of various inflammatory and autoimmune disorders.[29] It binds to its receptors (TNFR1 and TNFR2), triggering a signaling cascade that activates NF-κB and induce iNOS expression, therefore amplifying the inflammatory response.[30] Given that acupuncture-induced BP reduction is systemic in nature, we assessed TNF-α expression both locally and systemically. While local TNF-α showed a modest increase, systemic levels rose significantly, accompanied by a decline in IL-1β and TGF-β. These opposing trends suggest a nuanced balance between pro-inflammatory (TNF-α) and anti-inflammatory (IL-1β, TGF-β) responses. Liu et al, demonstrated that the critical role of the vagal-adrenal axis in mitigating systemic inflammation following acupuncture at ST36. Moreover, it is well known that inflammation and hypertension are closely linked, with chronic inflammation contributing to vascular damage, endothelial dysfunction, and increased blood pressure. Reducing inflammation may attenuate the production of angiotensin II, a potent vasoconstrictor, and thereby promoting vasodilation and lowering blood pressure. In clinical practice, acupuncture-induced blood pressure reduction is associated with a decrease in sympathetic nervous system activity.[31] The antihypertensive effect is likely mediated by the reduction in sympathetic excitation through the dual effect on inflammatory of ST36.

A key insight from the transcriptomic data was the elevated iNOS expression, a known mediator of inflammation and immune activation. iNOS is not constantly present in cells, and is only induced or stimulated in the context of inflammation.[32,33] Previous research has shown that the transcriptional regulation of iNOS is typically triggered by pro-inflammatory cytokines such as TNF-α, IL-1 and IFN-γ.[34–36] In our data, the expression levels of inflammatory factors were significantly increased. The manipulation technique (lifting, thrusting, twisting, and rotating) applied to ST36 likely damaged the local skin and muscle, causing focal inflammation. This localized pro-inflammatory microenvironment can induce iNOS expression, increasing NO release and subsequently promoting vasodilation. As shear stress and tissue stretch accumulate from local vasodilation, eNOS may also be activated, further amplifying NO production and contributing to systemic hypotension.[37] Prior studies have confirmed that NO plays a central role in acupuncture-induced vasodilation in both animals and humans, with elevated NO production linked to BP reduction.[38] Several investigations have specifically demonstrated the involvement of NO released from vascular endothelial cells to the cutaneous vasodilation triggered by acupuncture stimulation.[12,39] Correspondingly, we found that pharmacological inhibition using L-NAME effectively abolished the hypotensive response to ST36 stimulation, underscoring the pivotal involvement of NO-dependent pathways in mediating acupuncture-induced hypotension. Although L-NAME inhibits both iNOS and endothelial nitric oxide synthase (eNOS), future investigations are needed to dissect their individual contributions more precisely.

Furthermore, the interplay between iNOS and eNOS appears crucial in this process. The lifting-thrusting and twisting-rotating techniques at ST36 also generated mechanical signal transduction and connective tissue deformation, leading to shear stress on local vessels. Hemodynamic shear stress is a potent physiological regulator of eNOS, resulting in rapid increases in NO production.[40] While NO is a potent vasodilator, it exerts minimal effects on heart rate and contractility, implying that additional factors coexisting with NO may influence the cardiac response. Nonetheless, our findings highlight the iNOS-eNOS interplay as central to the observed vasodilatory and hypotensive effects of acupuncture.

There are several limitations to this study. First, in clinical practice, acupuncture is typically administered over several weeks, whereas in this study, MA was applied only once for 5 minutes. Thus, the effects on BP and heart rate may differ with prolonged intervention. Second, the precise mechanisms by which local inflammation at the acupoint elevates serum TNF-α levels require further elucidation. Lastly, conducting MA on conscious animals would better simulate the physiological conditions experienced by humans. Future research should also explore the long-term effects of repeated MA at ST36 and further elucidate the signaling pathways involved in its cardiovascular effects, including the use of specific iNOS inhibitors or TNF-α blockade.

Conclusion

Our study demonstrated that MA at ST36 significantly lowered BP, manifested by increased peripheral blood flow and decreased stroke volume and VTI of the femoral artery. This pronounced vasodilation in response to acupuncture is likely mediated by upregulation of iNOS and subsequent NO production from lifting-thrusting and twisting-rotating technique. The use of an iNOS inhibitor effectively blocked the hypotensive effect. Further research into the complex functions of iNOS is essential to fully understand the mechanisms underlying acupuncture's effects on cardiovascular health and to optimize its therapeutic potential. Our results suggest that acupuncture at ST36 can lower blood pressure in healthy rats, pointing to a potential benefit for individuals at risk of hypertension. In clinical practice, with optimized treatment duration and stimulation intensity, acupuncture's localized effect could provide a complementary or alternative approach, particularly for patients who do not respond well to conventional therapies.

Abbreviations

ST36, Acupoint Zusanli; MA, manual acupuncture; BP, blood pressure; ECG, electrocardiogram; HRV, heart rate variability; LSCI, laser speckle contrast imaging; WB, Western blotting; LF/HF, low-/high-frequency; TNF-α, tumor necrosis factor-alpha; NOS, nitric oxide synthase; NO, nitric oxide; L-NAME, L-NG-Nitro arginine methyl ester; EA, electroacupuncture; LVP, left ventricular pressure; LF, low frequency; HF, high frequency; VTI, velocity time integral; CO, cardiac output; TH, Tyrosine hydroxylase; p-TH, phosphorylated Tyrosine hydroxylase; MBP, Mean blood pressure; LVEDP, Left ventricular end systolic pressure; LVESP, Left ventricular end systolic pressure; DEGs, differentially expressed genes; lL-1β, Interleukin-1 beta; lL-10ra, Interleukin 10 receptor alpha; lL-17r, Interleukin 17-receptor E; lL-1rl1, Interleukin 1 receptor-like 1; Ccl-2, C-C motif chemokine ligand-2; Ccl-22, C-C motif chemokine ligand-22; Cxcl1, C-X-C motif chemokine ligand 1; Cxcl-2, C-X-C motif chemokine ligand-2. TGF-β, Transforming growth factor-β; IL-6, Interleukin-6. GSEA, Gene Set Enrichment Analysis. RMSSD, root mean square of successive difference.

Data Sharing Statement

The datasets used and/or analyzed during the current study are available from the corresponding author on reasonable request.

Ethics Approval and Consent to Participate

All procedures were approved by the Ethics Committee for Animal Care and Use in Chengdu University of Traditional Chinese Medicine, China (2018-11), and all procedures were conducted in accordance with the guidelines of the National Institutes of Health Animal Care and Use Committee. No human studies were carried out by the authors of this article.

Acknowledgment

We are grateful to the authors and patients of all the articles.

Funding

This work was supported by the National Natural Science Foundation of China (No. 81904306, 82274414), the National Key R&D Program of China (No. 2022YFC3500703), National Natural Science Foundation of Sichuan (2024NSFSC2118), and Sichuan Science and Technology Program (2020YFH0115).

Disclosure

The authors report no conflicts of interest in this work.

References

1. Flachskampf FA, Gallasch J, Gefeller O, et al. Randomized trial of acupuncture to lower blood pressure. *Circulation*. 2007;115(24):3121–3129. doi:10.1161/CIRCULATIONAHA.106.661140
2. Yin C, Seo B, Park H-J, et al. Acupuncture, a promising adjunctive therapy for essential hypertension: a double-blind, randomized, controlled trial. *Neurological Res*. 2007;29(sup1):98–103. doi:10.1179/016164107X172220

3. Macklin EA, Wayne PM, Kalish LA, et al. Stop hypertension with the acupuncture research program (SHARP): results of a randomized, controlled clinical trial. *Hypertension*. 2006;48(5):838–845. doi:10.1161/01.HYP.0000241090.28070.4c
4. Kim HM, Cho SY, Park SU, et al. Can acupuncture affect the circadian rhythm of blood pressure? A randomized, double-blind, controlled trial. *J Altern Complement Med*. 2012;18(10):918–923. doi:10.1089/acm.2011.0508
5. Liu S, Wang Z, Su Y, et al. A neuroanatomical basis for electroacupuncture to drive the vagal–adrenal axis. *Nature*. 2021;598(7882):641–645. doi:10.1038/s41586-021-04001-4
6. Huang T, Zhang W, Jia S, et al. A transcontinental pilot study for acupuncture lifting-thrusting and twisting-rotating manipulations. *Evid Based Complement Alternat Med*. 2012;2012:157989. doi:10.1155/2012/157989
7. da Silva MA, Dorsher PT. Neuroanatomic and clinical correspondences: acupuncture and vagus nerve stimulation. *J Altern Complement Med*. 2014;20(4):233–240. doi:10.1089/acm.2012.1022
8. Y-t K, Kanneganti A, Nothnagle C, et al. Microchannel electrode stimulation of deep peroneal nerve fascicles induced mean arterial depressor response in hypertensive rats. *Bioelectron Med*. 2015;2:55–62. doi:10.15424/bioelectronmed.2015.00001
9. Friedemann T, Li W, Wang Z. Inhibitory regulation of blood pressure by manual acupuncture in the anesthetized rat. *Auton Neurosci*. 2009;151 (2):178–182. doi:10.1016/j.autneu.2009.05.254
10. H-s B, A-s S, S-u P, et al. Effects of acupuncture at ST36 on blood pressure and endothelial dependent vasodilation in hypertensive patients. *J Int Korean Med*. 2008;29(3):657–665.
11. Severcan Ç, Cevik C, Acar HV, et al. The effects of acupuncture on the levels of blood pressure and nitric oxide in hypertensive patients. *Acupunct Electrother Res*. 2013;37(4):263–275. doi:10.3727/036012912X13831831256320
12. Tsuchiya M, Sato EF, Inoue M, Asada A. Acupuncture enhances generation of nitric oxide and increases local circulation. *Anesthesia Analg*. 2007;104(2):301–307. doi:10.1213/01.ane.0000230622.16367.fb
13. Förstermann U, Sessa WC. Nitric oxide synthases: regulation and function. *Eur Heart J*. 2012;33(7):829–837. doi:10.1093/eurheartj/ehr304
14. Pfeiffer S, Leopold E, Schmidt K, Brunner F, Mayer B. Inhibition of nitric oxide synthesis by NG-nitro-L-arginine methyl ester (L-NAME): requirement for bioactivation to the free acid, NG-nitro-L-arginine. *Br J Pharmacol*. 1996;118(6):1433–1440. doi:10.1111/j.1476-5381.1996.tb15557.x
15. Lo H-C, Hung C-Y, Huang F-H, Su T-C, Lee C-H. The nitric oxide synthase inhibitor NG-nitro-L-arginine methyl ester diminishes the immunomodulatory effects of parental arginine in rats with subacute peritonitis. *PLoS One*. 2016;11(3):e0151973. doi:10.1371/journal.pone.0151973
16. Kopincová J, Púzserová A, Bernátová I. L-NAME in the cardiovascular system—nitric oxide synthase activator? *Pharmacol Rep*. 2012;64 (3):511–520. doi:10.1016/S1734-1140(12)70846-0
17. Kimura K, Takeuchi H, Yuri K, Wakayama I. Inhibition of nitric oxide synthase attenuates cutaneous vasodilation during warm moxibustion-like thermal stimulation in humans. *J Altern Complementary Med*. 2012;18(10):965–970. doi:10.1089/acm.2011.0433
18. Wang SJ, Zhang YP, Candiotti KA. Effects of electroacupuncture on pain sensation in a rat model of hyperalgesia with nicotine dependence. *Neural Regen Res*. 2022;17(4):905–910. doi:10.4103/1673-5374.322477
19. Li J, Peng C, Lai D, et al. PET-CT and RNA sequencing reveal novel targets for acupuncture-induced lowering of blood pressure in spontaneously hypertensive rats. *Sci Rep*. 2021;11(1):10973. doi:10.1038/s41598-021-90467-1
20. Kim D, Paggi JM, Park C, Bennett C, Salzberg SL. Graph-based genome alignment and genotyping with HISAT2 and HISAT-genotype. *Nature Biotechnol*. 2019;37(8):907–915. doi:10.1038/s41587-019-0201-4
21. Pertea M, Pertea GM, Antonescu CM, Chang T-C, Mendell JT, Salzberg SL. StringTie enables improved reconstruction of a transcriptome from RNA-seq reads. *Nature Biotechnol*. 2015;33(3):290–295. doi:10.1038/nbt.3122
22. Fu S-P, He S-Y, Xu B, et al. Acupuncture promotes angiogenesis after myocardial ischemia through H3K9 acetylation regulation at VEGF gene. *PLoS One*. 2014;9(4):e94604. doi:10.1371/journal.pone.0094604
23. Xu S, Hu E, Cai Y, et al. Using clusterProfiler to characterize multiomics data. *Nat Protoc*. 2024;19(11):3292–3320. doi:10.1038/s41596-024-01020-z
24. Yu G. Enrichplot: visualization of functional enrichment result. *R Package Version*. 2021;1(2).
25. Yao H, Fu X, Xu Q, et al. The macrophages regulate intestinal motility dysfunction through the PGE2 Ptger3 axis during Klebsiella pneumonia sepsis. *Front Immunol*. 2023;14:1147674. doi:10.3389/fimmu.2023.1147674
26. Xin JJ, Gao JH, Wang YY, et al. Antihypertensive and antihypertrophic effects of acupuncture at pc6 acupoints in spontaneously hypertensive rats and the underlying mechanisms. *Evid Based Complement Alternat Med*. 2017;2017:9708094. doi:10.1155/2017/9708094
27. Cui X, Sun G, Cao H, et al. Referred somatic hyperalgesia mediates cardiac regulation by the activation of sympathetic nerves in a rat model of myocardial ischemia. *Neurosci Bull*. 2022;38(4):386–402. doi:10.1007/s12264-022-00841-w
28. Cao X, Lu S, Ohara H, et al. Beneficial and adverse effects of electro-acupuncture assessed in the canine chronic atrio-ventricular block model having severe hypertension and chronic heart failure. *Acupunct Electrother Res*. 2015;40(2):87–99. doi:10.3727/036012915x14381285982886
29. D-i J, Lee A-H, Shin H-Y, et al. The role of tumor necrosis factor alpha (TNF-α) in autoimmune disease and current TNF-α inhibitors in therapeutics. *Int J mol Sci*. 2021;22(5):2719. doi:10.3390/ijms22052719
30. Ruiz A, Palacios Y, Garcia I, Chavez-Galan L. Transmembrane TNF and its receptors TNFR1 and TNFR2 in mycobacterial infections. *Int J mol Sci*. 2021;22(11):5461. doi:10.3390/ijms22115461
31. Li P, Tjen ALSC, Cheng L, et al. Long-lasting reduction of blood pressure by electroacupuncture in patients with hypertension: randomized controlled trial. *Med Acupunct*. 2015;27(4):253–266. doi:10.1089/acu.2015.1106
32. Zamora R, Vodovotz Y, Billiar TR. Inducible nitric oxide synthase and inflammatory diseases. *Mol Med*. 2000;6:347–373.
33. Anavi S, Tirosh O. iNOS as a metabolic enzyme under stress conditions. *Free Radic Biol Med*. 2020;146:16–35. doi:10.1016/j.freeradbiomed.2019.10.411
34. Sharma J, Al-Omran A, Parvathy S. Role of nitric oxide in inflammatory diseases. *Inflammopharmacology*. 2007;15:252–259. doi:10.1007/s10787-007-0013-x
35. Kleinert H, Art J, Pautz A. Regulation of the expression of inducible nitric oxide synthase. *Nitric Oxide*. 2010;211–267.
36. Pautz A, Art J, Hahn S, Nowag S, Voss C, Kleinert H. Regulation of the expression of inducible nitric oxide synthase. *Nitric Oxide*. 2010;23 (2):75–93. doi:10.1016/j.niox.2010.04.007

37. Erkens R, Suvorava T, Kramer CM, Diederich LD, Kelm M, Cortese-Krott MM. Modulation of local and systemic heterocellular communication by mechanical forces: a role of endothelial nitric oxide synthase. *Antioxid Redox Signal*. 2017;26(16):917–935. doi:10.1089/ars.2016.6904
38. Ma S-X. Neurobiology of acupuncture: toward CAM. *Evid Based Complementary Altern Med*. 2004;1(1):41–47. doi:10.1093/ecam/neh017
39. Loaiza LA, Yamaguchi S, Ito M, Ohshima N. Electro-acupuncture stimulation to muscle afferents in anesthetized rats modulates the blood flow to the knee joint through autonomic reflexes and nitric oxide. *Auton Neurosci*. 2002;97(2):103–109. doi:10.1016/S1566-0702(02)00051-6
40. Sprague B, Chesler NC, Magness RR. Shear stress regulation of nitric oxide production in uterine and placental artery endothelial cells: experimental studies and hemodynamic models of shear stress forces on endothelial cells. *Int J Dev Biol*. 2010;54(2–3):331. doi:10.1387/ijdb.082832bs